Environmental Science: Atmospheres

ROYAL SOCIETY OF CHEMISTRY

PAPER

View Article Online
View Journal | View Issue

Check for updates

Cite this: *Environ. Sci.: Atmos.*, 2023, **3**, 1212

Negligible increase in indoor endotoxin activity by 222 nm far-UVC illumination on bioaerosols†

Zhancong Liang, Tim Yiu Cheung, Wing Lam Chan, Chee Kent Lim, Alvin. C. K. Lai, Patrick. K. H. Lee and Chak K. Chan ‡*

Far-UVC irradiation (222 nm) is an emerging approach for disinfection due to its effectiveness and potentially harmless nature to humans by direct irradiation compared with other UV wavelengths. However, the indirect risk caused by 222 nm irradiance, such as changes in the inhalation hazard of irradiated bioaerosols, is poorly studied. In particular, Gram-negative bacteria (GNB) lysis releases endotoxins, which can cause respiratory diseases *via* inhalation. Herein, we measured the endotoxin activity of illuminated GNB bioaerosols in a chamber using the limulus amebocyte lysate (LAL) assay. A 4-fold higher endotoxin activity ratio (EAR) of the UV-irradiated cells to fresh cells was found in the GNB bioaerosols illuminated by 222 nm than 254 nm, which can be explained by the different inactivation mechanisms. Compared with 254 nm, 222 nm illumination excited the cell membrane components (*e.g.*, proteins) more effectively, leading to the formation of more reactive oxygen species (ROS) and membrane damage, followed by exposing lipid A to release the free-endotoxins into the aqueous environment of the aerosols. The increase in EAR, membrane damage, and ROS level at 222 nm were significantly higher than at 254 nm ($p < 0.05$). The EAR increased linearly with the UV dose up to 50 mJ cm^{-2}. The EAR increase rate constant (k_{EAR}) was insensitive to the KCl concentration in the aerosol, but it decreased by more than 80% when the droplets became solid particles. At a 222 nm UV dose of 50 mJ cm^{-2}, the increase in indoor endotoxin activity due to illuminated GNB in typical indoor environments was estimated to be 3 orders of magnitude lower than the pre-existing endotoxin activity. Thus, our work suggests a negligible increase in endotoxic risk due to 222 nm indoor disinfection.

Received 25th April 2023
Accepted 2nd July 2023

DOI: 10.1039/d3ea00059a

rsc.li/esatmospheres

Environmental significance

Humans suffer from significant hazards of respiratory diseases *via* airborne transmission, especially indoors. Recently, far-UVC at 222 nm has become increasingly popular due to its claimed harmless nature to the human eye and skin by direct irradiation, besides its high efficiency in disinfecting pathogens. This technique has high potential to afford effective indoor disinfection. However, in addition to direct irradiation on humans, the "invisible" risks, such as that *via* the inhalation of airborne particles, should be carefully assessed. By investigating the endotoxin activity of irradiated bioaerosols at 222 nm, this study provides new insights into the impact of far-UVC applications on indoor air quality.

1. Introduction

Increasing evidence shows that COVID can be airborne and transmitted *via* aerosol,[1–4] which suggests an exposure risk from respiratory aerosol and droplets exhaled by pathogen carriers. Therefore, techniques are urgently needed for the effective disinfection of high human-density areas, *i.e.*, a sufficiently high log reduction in pathogen viability.[5] Ultra-violet (UV) illumination is one of the most popular approaches in disinfection, especially during the COVID-19 epidemic.[6–8] Conventional UV disinfection mainly relies on 254 nm UVC, which can achieve around 99% inactivation of bacteria and virus bioaerosols using a UV dose of about 1 mJ cm^{-2}.[9,10] However, 254 nm UVC can deeply penetrate human tissues and lead to severe diseases such as skin cancer and keratitis, limiting its application to no-human zones only.[11,12]

Different from UVC at 254 nm, far-UVC at 222 nm has a transmittance of ≤1% in keratin and corneal, given that light can be effectively absorbed by proteinaceous matter.[13–18] Thus, it may not penetrate the stratum corneum of human skin and the cornea of the human eye, protecting humans from UV-induced diseases.[16,19] Currently, the exposure limit for 222 nm far-UVC light is set at 240 J m^{-2} by the International Commission on Non-Ionizing Radiation Protection (ICNIRP), which is 4-fold

School of Energy and Environment, City University of Hong Kong, 83 Tat Chee Avenue, Kowloon, Hong Kong, China. E-mail: chak.chan@kaust.edu.sa; chak.k.chan@cityu.edu.hk

† Electronic supplementary information (ESI) available. See DOI: https://doi.org/10.1039/d3ea00059a

‡ Current address: Division of Physical Science and Engineering, King Abdullah University of Science and Technology, Thuwal, 23955-6900, Saudi Arabia.

higher than that of 254 nm.[20] Besides, far-UVC light may provide more permanent disinfection than 254 nm UV light, given that it inhibits the re-activation of pathogens, which occurs under other light sources.[21] Many emerging studies have shown the excellent efficiency of far-UVC for the inactivation of pathogens, including SARS-CoV-2.[22] Considering these benefits, 222 nm far-UVC products have been proposed to be an effective disinfection tool, even with direct exposure to humans and pets, while UVC products only aim at disinfection without this exposure.[4,21–23]

The proposed harmless nature of far-UVC irradiation on the human body (though still controversial[24]) makes it increasingly popular for indoor applications.[16,19] Nevertheless, it is still unclear if there are any other environmental risks during 222 nm disinfection, besides direct irradiation. For example, endotoxins, also known as LPS (lipopolysaccharides), are a component of the cell wall of Gram-negative bacteria (GNB), which can be released during cell lysis.[25–27] Airborne endotoxins may exist as shed membrane complexes (free endotoxins) or bound-endotoxins when combined with other biological and non-biological particles (*e.g.*, on the outer bacterial membrane but detectable by endotoxin assays).[28] Free-endotoxins have higher activity and toxicity than bound-endotoxins.[29] It has been reported that the LD50 of lipopolysaccharides (LPS, purified derivatives of endotoxins) by inhalation in mice ranges from 0.5 to 5 mg kg^{-1}.[30] Inhalation of particulate endotoxins is considered to be one of the leading causes of respiratory diseases, including sensitization, allergic asthma, and other immune responses.[26,31–33] Besides, the inhaled particulate endotoxins may deposit in the human lungs, leading to long-term health effects.[34]

It has been reported that UVC illumination of a GNB aqueous suspension induced an increase in endotoxin activity with UV dose.[35] Given that the energy of UVC photons is not high enough to break the molecular structure of endotoxins, a high level of endotoxin activity was retained.[36] Alternatively, Wang *et al.* reported that UVD (185 nm) illumination of bioaerosols could decrease the total endotoxin activity, which was attributed to the generation of ozone to degrade the endotoxin molecules.[36] 222 nm far-UVC has photon energy between that of UVC and UVD. However, despite its increasing utilization, how far-UVC irradiation impacts the endotoxin activity of bioaerosol remains unexplored.

In this work, we investigated the changes in endotoxin activity during far-UVC illumination of a GNB bioaerosol. Firstly, we compared the endotoxins released from *Escherichia coli* (*E. coli*) under 222 nm far-UVC with 254 nm UVC illumination as in conventional UV disinfection. The endotoxin activity was determined using the specific limulus amebocyte lysate (LAL) assay. The amount of endotoxins in a sample is proportional to the amount of color change that occurs when mixed with the lysate.[37] We focused on *E. coli*, an airborne GNB found indoors[38,39] and widely adopted in airborne endotoxin-related research.[36,40] We also used another atmospheric-relevant GNB, *i.e.*, *Pseudomonas putida*,[41,42] to provide additional data supporting the key results obtained for *E. coli*. The experiments using DNA dyes and reactive oxygen species (ROS) probes shed light on the potentially different mechanisms between far-UVC- and UVC-induced endotoxin release during cell inactivation. Then, the effects of parameters such as UV dose, solute concentration and phase state of the aerosol particles on the endotoxin release were also explored. Finally, we evaluated the impact of 222 nm far-UVC disinfection on the endotoxic risk in indoor air application. We introduced the basic experimental design in Section 2 and more detailed experimental information can be found in Text S1–S7.†

2. Materials and methods

2.1 Aging of the bioaerosol

The preparation of *E. coli* BW25113 can be found in the ESI (Text S1†). The UV-aging experiments of bioaerosol were performed in a ~0.5 m^3 Teflon chamber with a 222 nm KrCl* excimer (30 W, DM222, Daylight) or 254 nm Hg (30 W, TUV, Philip) lamp installed on the top and the bottom, respectively (Fig. S1†). Briefly, the chamber was first filled with HEPA-sterilized zero air. A cleaned 24-jet collision-type nebulizer (BGI Inc.) was used to aerosolize bacteria from suspensions of 10^7 CFU mL^{-1} cells in pyrogen-free water or 2 g L^{-1} [KCl] solution (comparable to the solute concentration in artificial saliva)[43] before UV illumination. Four bladeless fans were used to enhance the air mixing inside the chamber. A stream of HEPA-sterilized zero air was introduced to keep the RH within 5% of that before nebulization. The relative humidity (RH) was measured by a temperature and humidity meter (HM170, Vaisala), and the temperature was 23 ± 2.4 °C. The spectra of the light tubes are shown in the ESI (Fig. S2†). The 222 nm light tubes stabilized instantly after they were turned on, but the 254 nm light tubes took around 30 min to stabilize. The average light irradiance of the 254 nm lamps was comparable with the 222 nm lamps by using different numbers of lamps. We conducted symmetrical 16-point grid measurements of UV irradiance at six equally spaced vertical levels inside the chamber and calculated the average, as described by Lu *et al.*[44] The UV dose on the bioaerosol was estimated by the product of the average UV irradiance and the illumination time of the bioaerosol.[45] Besides UVs, we also aged the bioaerosol by ozone given that 222 nm far-UVC was reported to generate ozone.[46] A flow of O_3 (~0.01 L min^{-1}) was generated by passing O_2 (99.995%, Linde) to an O_3 generator (Model 610, Jelight Company Inc, USA). Then, we diluted the ozone using a two-stage dilution system[47] and introduced it into the chamber after mixing with the zero air. An ozone monitor (106-L, 2B Technology) was used to measure the ozone concentration at the exhaust of the chamber.

2.2 Measurement of the endotoxin activity

The aerosolized bacteria were sampled in a PBS solution using a Spot Sampler (Aerosol Devices Inc.) after 0, 2, 4, 6, 8, and 10 min of UV illumination. The Spot Sampler affords a high collection efficiency of viral bioaerosol particles based on the condensational growth of the particles followed by particle-to-liquid sampling.[48]

The endotoxin activity (EU per mL) of the collected sample was determined using the specific LAL assay (Bioendo, China) (Text S2†). Endotoxin activity describes the total reactivity of endotoxins with LAL to reflect their hazard level.[35,49,50] Free-endotoxins have higher reactivity than bound-endotoxins.[35] Briefly, the assay reacts with endotoxins to form light-absorbing compounds. In the assay-sample mixture, the endotoxin activity was linearly correlated with the light absorption intensity at 545 nm, which was measured using a molecule fluoroscope (SpectraMax M2e).

Given that our observation includes the conversion from bound-endotoxin to free-endotoxin, we did not report the absolute endotoxin concentration, which needs to assume comparable reactivity of individual endotoxin molecules. We used the endotoxin activity ratio (EAR) of the UV-irradiated cells to that conditioned in the dark to show the changes in endotoxin activity due to UV-irradiation. It should be noted that the EAR reported in this study refers to total endotoxin activity (*i.e.*, the sum of free-endotoxin and bound-endotoxin activity). The activities of total endotoxin and free-endotoxin were determined by applying the LAL assay to the cell suspension and the filtrate using 0.22 μm PTFE filters, respectively, at different intervals during illumination by 222 nm or 254 nm light. We assumed that the free-endotoxins penetrated the filter.[29,36,51] The bound-endotoxin activity was determined by subtracting the free-endotoxin activity from the total endotoxin activity. All the materials used were pyrogen-free.

2.3 The relative viability, membrane damage and ROS generation

The relative viability (RV) of bacteria, which is defined as the viable cell concentration with UV to that without, was determined by the plate-counting method, as described in our previous work.[43] We incubated the collected samples after spreading on a plate and counted the colony numbers. Then, we estimated the initial cell concentration (*i.e.*, before UV on) in the chamber to be 10^6 CFU m^{-3} by dividing the colony number by the volume of air we sampled. To reduce the wall loss of the bioaerosols, we used a short sampling time of 5 min. Hence, a high concentration of airborne cells was used to satisfy the detection limit of assays. The cell damage and intracellular ROS level were characterized by the fluorescent dyes propidium iodide, SYBR® Green I, and 2′,7′-dichlorodihydrofluorescein diacetate (H2DCFDA). A detailed description can be found in the ESI (Text S3 and S4†). All the uncertainties reported herein were from triplicate measurements.

2.4 Statistical analysis

All data in the figures are presented as mean ± standard deviation (SD). The change in the inactivation value and ozone concentration between the different experimental groups over the experimental period was compared using the repeated-measure analysis of variance (ANOVA) (Igor Pro 8). The differences in the results between the 222 nm- and 254 nm-irradiated samples were analyzed by one-way ANOVA. A p-value of <0.05 was regarded as statistically significant.

3. Results and discussions

3.1 Increase in endotoxin activity upon UV illumination

Fig. 1a shows the EAR as a function of illumination time. At 222 nm illumination, the EAR exhibited a linear increase with time to around 16 at 10 min. At 254 nm illumination, the EAR increased but much slower (*i.e.*, only reached ~3.7 after 10 min). This difference indicates that the endotoxic risk under a comparable UV dose (42 mJ cm^{-2} at 10 min) is around 4 times under 222 nm than 254 nm. A negligible increase in endotoxin activity was observed in the dark (Fig. S3†).

The increase in EAR upon photochemical aging can be attributed to the lysis of cells that release free-endotoxins,[52] which have higher reactivity than bound-endotoxins. As shown in Fig. 1b, the fraction of free-endotoxins increased significantly from 0.04 to 0.76 and 0.98 after 2 min and 4 min of 222 nm illumination, respectively, and remained high for a longer illumination time. In contrast, the fraction of free-endotoxins in the 254 nm-illuminated sample only reached ~0.23 after 10 min of illumination.

The bound-endotoxin activity of the 222 nm-irradiated cells decreased, due to the conversion to free-endotoxins. Similar to that reported by Huang *et al.*,[49] the activity of bound-endotoxins (as well as the total activity of endotoxins) increased after 254 nm aging (Fig. S4†). Endotoxins are composed of O-specific antigen (the outermost component exposed to the environment), core polysaccharides (located at the middle of the endotoxins), and lipid A (embedded in the cell membrane but

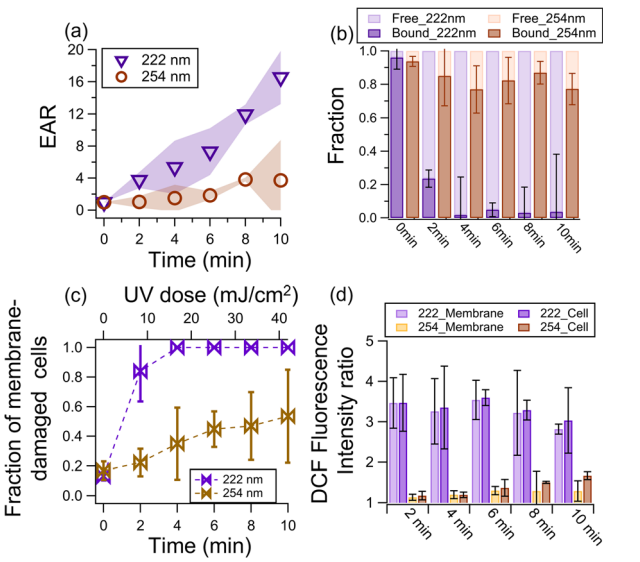

Fig. 1 (a) Total endotoxin activity ratio (EAR) as a function of illumination time. (b) Fractions of free- and bound-endotoxin activity of the total endotoxin activity. (c) Fraction of membrane-damaged cells as a function of illumination time. (d) DCF fluorescence intensity ratio of illuminated samples to fresh samples as a function of illumination time. 222_Membrane and 222_Cell denote the membrane components and intact cells under 222 nm irradiation, respectively. The one-way ANOVA test indicates that at $\alpha = 0.05$, the 222 nm and 254 nm data shown in (a–d) have p from 3×10^{-7} to 0.43. Thus, the 222 nm data were considered statistically different from the 254 nm data.

has been considered as the endotoxic component).[53,54] Lipid A is the main endotoxic unit of endotoxin molecules,[55] and it was no longer protected by the UV exposed and damaged membrane although the endotoxin unit was still bound to the cell. Consequently, the activity of the cell-bound endotoxin increased.

3.2 Bacterial inactivation mechanism affects endotoxin release

The bacteria showed RV reduction to below the detection limit after 10 min of 222 nm or 254 nm illumination. Nevertheless, the endotoxin activity was 5-fold higher at 222 nm than that at 254 nm. The steady-state ozone concentrations upon 222 nm and 254 nm illumination were low, *i.e.*, 3.6 ± 1.1 ppb and 2.4 ± 2.2 ppb, respectively. The control experiments using 10 ppb ozone in the dark only showed an EAR of 1.3 after 10 min, indicating the minor role of ozone in disinfection. Therefore, the discrepancy in endotoxin activity was likely due to the different inactivation mechanisms between far-UVC and UVC.

Intercellular proteins and some lipids have the maximum light absorbance at around 220 nm, while that of nucleic acid is at 260 nm.[56,57] The excitation energy for lipids and proteins on the bacterial membrane was reported to be 5.4–6.2 eV and 4.4–4.8 eV, respectively,[58–60] which is comparable to or lower than the photon energy at 222 nm (5.59 eV). Thus, 222 nm illumination can excite these membrane chromophores to trigger ROS generation,[13,61] which then damaged the DNA and membrane (Fig. 2a).[56,62–64] The generation of ROS may be triggered by photolysis and photosensitization of the excited membrane components, depending on their complex bond dissociation energy.[58,65] In contrast, 254 nm UVC disinfection mainly relies on degrading the DNA or forming DNA-pyrimidine dimers, which inhibit transcription and translation (Fig. 2b).[64,66] The low light absorption ability of membrane components at 254 nm limits the effectiveness of membrane degradation.[56,57]

The fraction of cells with damaged membranes abruptly increased from 0.2 to around 0.8 and 1 after 2 and 4 min of 222 nm irradiation, respectively. In contrast, the membrane-damaged cell fraction only increased to 0.47 after 10 min of 254 nm illumination (Fig. 1c). To shed light on the potential mechanisms of membrane damage, we determined the ROS level in the samples using the H_2DCFDA probe of fluorescent DCF to obtain the DCF fluorescence intensity ratio (FIR) of illuminated samples to fresh samples as an indicator of the ROS level.[67,68] A larger FIR indicates a higher ROS level after illumination. The FIR reached ~3.5 after 2 min of 222 nm irradiation, which gradually decreased to around ~2.8 at 10 min. The decrease in ROS level was probably due to the photolytic consumption of the light-absorbing compounds that generate ROS. In contrast, the maximum FIR was only 1.3 at 254 nm irradiance. Besides, there are more substrates (*e.g.*, membrane and proteins) that could be excited and generate ROS at 222 nm irradiance. Also, the 222 nm light could also effectively inactivate the enzymes that generate a membrane potential to resist ROS.[56] Consequently, the cells illuminated at 222 nm exhibited a much larger increase in ROS level. The one-way ANOVA test indicated that at $\alpha = 0.05$, the 222 nm and 254 nm data shown in Fig. 1a–d have a p of less than 0.05 (*i.e.*, $3 \times 10^{-7} - 0.43$).

Our findings are consistent with a study in which far-UVC illumination resulted in 100% and 80% more cells with elevated ROS levels and cells with membrane permeabilization, respectively, than UVC of the same dose (80 mJ cm^{-2}).[64] Under 222 nm irradiation, the ROS levels generated by the membrane component (222_Membrane, Text S5†) contributed to 98% of the ROS levels generated by the cells (222_Cell, Fig. 1d). Although the ROS level of 254_M was initially (*i.e.*, upon 1 min of irradiance) comparable to that of the cells (254_Cell), its contribution to 254_C decreased to 60% at 10 min, suggesting the increasingly important role of intracellular photochemistry. Taking all these together, we proposed that 222 nm irradiance excited the membrane components to generate more ROS than 254 nm, and these ROS damaged the membrane and exposed the lipid A of the bound-endotoxins and formed free-endotoxins. UVC irradiation also damages the cell membrane and wall of bacteria, causing them to rupture and release endotoxins into the air.[36] The 254 nm irradiation was mainly absorbed by the nuclei acids to generate ROS intercellularly (Fig. 1d) rather than on the membrane. However, these ROS generated within the cell could still oxidize the membrane to release free endotoxins, given that membrane damage was also found in the 254 nm-irradiated cells (Fig. 1c). It is also possible that the chemical transformation (*e.g.*, functionalization) of the free-endotoxins changed their activity.[69,70]

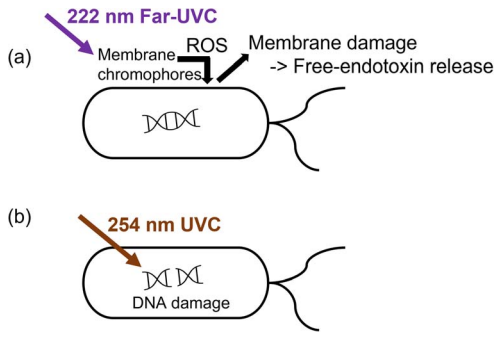

Fig. 2 Possible different inactivation mechanisms between (a) 222 nm and (b) 254 nm that affect the increase in EAR.

3.3 Effects of UV dose, RH and particle phase states

The average UV irradiance to the chamber was adjusted by the number of lamps. The data of low UV irradiance (35 μW cm^{-2}), which is commonly applied for airborne disinfection, was also included.[19,71,72] We found that for all UV irradiance, the endotoxin activity ratio linearly increased with the UV dose ($R^2 = 0.74$), supporting that the release of endotoxins was due to photochemistry (Fig. 3a). The good linearity of all the data at different light intensities indicates that the UV irradiance and time are interchangeable in terms of equivalent dosage for endotoxin release.

Human saliva is a very diluted aqueous solution. However, after exhalation, the water from the droplets and aerosol

particles will evaporate until it equilibrates with the ambient water vapor, or the particles undergo a phase transition to form solids.[73–75] During evaporation, the concentrations of cells and solute increase. Fig. 3b shows the EAR increase rate constant (k_{EAR}) as a function of RH. Although the solute concentrations increased from 2 g L^{-1} at 98%RH to 660 g L^{-1} at 54% RH, the k_{EAR} remained almost constant (around 0.5 UV dose^{-1}).

Our previous work demonstrated that the RV of bacteria strongly depends on the solute concentration of the expiratory particles.[43] Specifically, an elevated solute concentration induces high osmotic stress on the cells. Water can be extracted from cells, leading to cellular atrophy and membrane damage after the osmotic stress exceeds a certain threshold.[76] The control experiments showed that the threshold of osmotic stress tolerance is around 6 g L^{-1} KCl (equivalent to an equilibrium [KCl] at approximately 98% RH, Fig. S8†). However, there were no significant changes in the k_{EAR} when the RH dropped to as low as 54%, suggesting that the osmosis-induced membrane damage has a negligible effect on endotoxin release.

At RHs below 50%, the k_{EAR} decreased to ~0.1 UV dose^{-1} under 222 nm illumination irrespective of RH. This observation is attributed to the crystallization of KCl, which occurs upon evaporation at RHs below 50%, irrespective of the cell concentration (Fig. S9 and Text S6†). The concentration effect no longer exists in crystalline particles, and the poor diffusion in the crystalline matrix greatly hinders chemical reactions.[77,78] Comparably low k_{EAR} values were found in the illuminated crystalline particles containing cells using a flow cell (Text S8†).

4. Environmental implications

In this work, we presented a rapid increase in the EAR of illuminated GNB under 222 nm far-UVC compared to 254 nm UVC, which is mainly attributed to the photoexcitation of some membrane components that induced the oxidation of bound-endotoxins to release free-endotoxins. We also conducted similar experiments using *Pseudomonas putida*, another GNB with atmospheric relevance (Fig. S10†).[41,42] It has been reported that a UV dose of ≤50 mJ cm^{-2} can lead to 4-log RV reductions of pathogenic bacteria such as Methicillin-Resistant *Staphylococcus aureus* (MRSA)[79,80] and viruses such as SARS-CoV-2 in the air and on surfaces.[15,71,81] This UV dose falls in the regime for a rapid increase in endotoxin activity due to GNB aging based on our results. Hence, evaluating this "invisible" health risk during 222 nm far-UVC disinfection is of great importance.

In typical indoor environments, the GNB concentration varies from 10 CFU m^{-3} in residential homes to 10^4 CFU m^{-3} in wet markets (Fig. S11†).[82–96] These GNB concentrations yield endotoxin activity (EA) of 5.3 × 10^{-4} to 2.7 × 10^{-1} EU per m^3, assuming an EA per GNB of 5.3 × 10^{-6} EU per CFU (Fig. S12†). Using a k_{EAR} of 0.5 UV dose^{-1} as a reference (Fig. 2b), the increase in EA due to 222 nm at a UV dose of 50 mJ cm^{-2} for an hour was only 10^{-4}–10^{-1} EU per m^3, which is approximately 3-orders of magnitude lower than the pre-existing EA without 222 nm irradiation (Fig. S13†).

Recent works have found that a low UV dose (*e.g.*, 2 mJ cm^{-2}) of 222 nm can afford effective inactivation of airborne microorganisms for indoor applications.[21,44,45] By using a well-controlled chamber system, our results suggest a negligible endotoxin release under this UV dose. We encourage further investigations on the variation in endotoxin level due to 222 nm in different natural indoor environments. Genetic analysis will provide more direct evidence of bacterial inactivation mechanisms by different UV treatments. Nevertheless, other 222 nm photochemistry that may lead to indoor air pollution should be further evaluated. Using a kinetic model, Peng *et al.* reported the enhanced formation of secondary organic aerosol (SOA) under 222 nm over 254 nm disinfection at a comparable virus removal efficiency and low ventilation rate.[97] This modelling was based on typical indoor air conditions without human activity. However, human activities such as bleaching emit many new pollutants (*e.g.*, HOCl), which have high light-absorbing ability at 222 nm and can trigger multiphase chemistry.[98,99] Future works are encouraged to explore atmospheric photochemistry in indoor environments initiated by 222 nm irradiance and its potential impacts on human health.

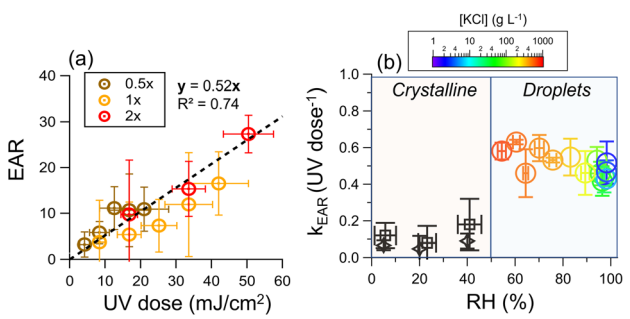

Fig. 3 (a) Endotoxin activity ratio as a function of UV dose, where 0.5×, 1×, and 2× represent the average UV irradiance of 35, 70, and 140 μW cm^{-2}, respectively. The bioaerosol was nebulized from water suspension. (b) Rate constant of the increase of endotoxin activity ratio as a function of RH. The [KCl] in the droplets (right region) was determined by hygroscopicity measurements at RH higher than efflorescence RH (Text S6, Fig. S5 and S6†). For an RH higher than 83%, which cannot be reached in the chamber, the results were obtained from illuminated aqueous suspension (Text S7 and Fig. S7†), and results of the illuminated crystalline particles were obtained from initially 2 g L^{-1} KCl droplets with 10^7 CFU mL^{-1} cells using a flow cell (black rhombuses, Text S8 and Fig. S5†) and a teflon chamber (black squares).

Author contributions

Zhancong Liang: conceptualization, organization, investigation, data analysis, writing – original draft writing – review & editing. Tim Yiu Cheung: investigation, writing – original draft writing. Wing Lam Chan: investigation, writing – original draft writing Chee Kent Lim: investigation, writing – original draft writing. Alvin. C. K. Lai: writing – original draft writing – review & editing. Patrick. K. H. Lee: writing – original draft writing – review & editing. Chak K. Chan: conceptualization, organization, investigation, data analysis, writing – original draft writing – review & editing.

Conflicts of interest

There are no conflicts to declare.

Acknowledgements

The work is supported by the Hong Kong Research Grants Council (R1016-20F, No. 11304121) and the National Natural Science Foundation of China (No. 42275104). We gratefully acknowledge the help from Dr Fengyu Qin from CityU in using the ultrasonic cell disruptor, and Dr Huihui Zhang from CityU and Mr Kai Wu from Daylight Inc. in the UV irradiance measurement of the 222 nm lamps.

References

1 L. C. Marr and J. W. Tang, A paradigm shift to align transmission routes with mechanisms, *Clin. Infect. Dis.*, 2021, **73**, 1747–1749.
2 K. A. Prather, L. C. Marr, R. T. Schooley, M. A. McDiarmid, M. E. Wilson and D. K. Milton, Airborne transmission of SARS-CoV-2, *Science*, 2020, **370**, 303–304.
3 L. Morawska and J. Cao, Airborne transmission of SARS-CoV-2: The world should face the reality, *Environ. Int.*, 2020, **139**, 105730.
4 L. Morawska, J. W. Tang, W. Bahnfleth, P. M. Bluyssen, A. Boerstra, G. Buonanno, J. Cao, S. Dancer, A. Floto and F. Franchimon, How can airborne transmission of COVID-19 indoors be minimised?, *Environ. Int.*, 2020, **142**, 105832.
5 G. Xiling, C. Yin, W. Ling, W. Xiaosong, F. Jingjing, L. Fang, Z. Xiaoyan, G. Yiyue, C. Ying, C. Lunbiao, Z. Liubo, S. Hong and X. Yan, *In vitro* inactivation of SARS-CoV-2 by commonly used disinfection products and methods, *Sci. Rep.*, 2021, **11**, 2418.
6 M. Raeiszadeh and B. Adeli, A critical review on ultraviolet disinfection systems against COVID-19 outbreak: applicability, validation, and safety considerations, *ACS Photonics*, 2020, **7**, 2941–2951.
7 E. A. Nardell, Air Disinfection for Airborne Infection Control with a Focus on COVID-19: Why Germicidal UV is Essential, *Photochem. Photobiol.*, 2021, **97**, 493–497.
8 C. P. Sabino, A. R. Ball, M. S. Baptista, T. Dai, M. R. Hamblin, M. S. Ribeiro, A. L. Santos, F. P. Sellera, G. P. Tegos and M. Wainwright, Light-based technologies for management of COVID-19 pandemic crisis, *J. Photochem. Photobiol., B*, 2020, **212**, 111999.
9 C.-Y. Lin and C.-S. Li, Control effectiveness of ultraviolet germicidal irradiation on bioaerosols, *Aerosol Sci. Technol.*, 2002, **36**, 474–478.
10 W. J. Snelling, A. Afkhami, H. L. Turkington, C. Carlisle, S. L. Cosby, J. W. Hamilton, N. G. Ternan and P. S. Dunlop, Efficacy of single pass UVC air treatment for the inactivation of coronavirus, MS2 coliphage and Staphylococcus aureus bioaerosols, *J. Aerosol Sci.*, 2022, **164**, 106003.
11 C. P. Sabino, F. P. Sellera, D. F. Sales-Medina, R. R. G. Machado, E. L. Durigon, L. H. Freitas-Junior and M. S. Ribeiro, UV-C (254 nm) lethal doses for SARS-CoV-2, *Photodiagn. Photodyn. Ther.*, 2020, **32**, 101995.
12 J. Glaab, N. Lobo-Ploch, H. K. Cho, T. Filler, H. Gundlach, M. Guttmann, S. Hagedorn, S. B. Lohan, F. Mehnke and J. Schleusener, Author Correction: Skin tolerant inactivation of multiresistant pathogens using far-UVC LEDs, *Sci. Rep.*, 2022, **12**, 1–3.
13 K. Narita, K. Asano, Y. Morimoto, T. Igarashi and A. Nakane, Chronic irradiation with 222-nm UVC light induces neither DNA damage nor epidermal lesions in mouse skin, even at high doses, *PLoS One*, 2018, **13**, e0201259.
14 S. Kaidzu, K. Sugihara, M. Sasaki, A. Nishiaki, T. Igarashi and M. Tanito, Evaluation of acute corneal damage induced by 222-nm and 254-nm ultraviolet light in Sprague–Dawley rats, *Free Radical Res.*, 2019, **53**, 611–617.
15 H. Kitagawa, T. Nomura, T. Nazmul, R. Kawano, K. Omori, N. Shigemoto, T. Sakaguchi and H. Ohge, Effect of intermittent irradiation and fluence-response of 222 nm ultraviolet light on SARS-CoV-2 contamination, *Photodiagn. Photodyn. Ther.*, 2021, **33**, 102184.
16 T. Fukui, T. Niikura, T. Oda, Y. Kumabe, H. Ohashi, M. Sasaki, T. Igarashi, M. Kunisada, N. Yamano and K. Oe, Exploratory clinical trial on the safety and bactericidal effect of 222-nm ultraviolet C irradiation in healthy humans, *PLoS One*, 2020, **15**, e0235948.
17 T. Fukui, T. Niikura, T. Oda, Y. Kumabe, A. Nishiaki, R. Kaigome, H. Ohashi, M. Sasaki, T. Igarashi and K. Oe, Safety of 222 nm UVC irradiation to the surgical site in a rabbit model, *Photochem. Photobiol.*, 2022, **98**(6), 1365–1371.
18 J. Cadet, Harmless effects of sterilizing 222-nm far-UV radiation on mouse skin and eye tissues, *Photochem. Photobiol.*, 2020, **96**, 949–950.
19 K. Sugihara, S. Kaidzu, M. Sasaki, S. Ichioka, Y. Takayanagi, H. Shimizu, I. Sano, K. Hara and M. Tanito, One-Year Ocular Safety Observation of Workers and Estimations of Microorganism Inactivation Efficacy in the Room Irradiated with 222-nm far Ultraviolet-C Lamps, *Photochem. Photobiol.*, 2023, **99**(3), 967–974.
20 K. Nield, CIE Position Statement on Ultraviolet (UV) Radiation to Manage the Risk of COVID-19 Transmission, *Light Eng.*, 2020, 4–8.
21 M. Buonanno, D. Welch, I. Shuryak and D. J. Brenner, Far-UVC light (222 nm) efficiently and safely inactivates airborne human coronaviruses, *Sci. Rep.*, 2020, **10**, 1–8.
22 H. Kitagawa, T. Nomura, T. Nazmul, K. Omori, N. Shigemoto, T. Sakaguchi and H. Ohge, Effectiveness of 222-nm ultraviolet light on disinfecting SARS-CoV-2 surface contamination, *Am. J. Infect. Control*, 2021, **49**, 299–301.
23 N. Hanamura, H. Ohashi, Y. Morimoto, T. Igarashi and Y. Tabata, Viability evaluation of layered cell sheets after ultraviolet light irradiation of 222 nm, *Regener. Ther.*, 2020, **14**, 344–351.
24 Q. Ong, W. Wee, J. Dela Cruz, J. W. R. Teo and W. Han, 222-Nanometer Far-UVC Exposure Results in DNA Damage and Transcriptional Changes to Mammalian Cells, *Int. J. Mol. Sci.*, 2022, **23**, 9112.

25 Y. Yue, H. Chen, A. Setyan, M. Elser, M. Dietrich, J. Li, T. Zhang, X. Zhang, Y. Zheng and J. Wang, Size-resolved endotoxin and oxidative potential of ambient particles in Beijing and Zurich, *Environ. Sci. Technol.*, 2018, **52**, 6816–6824.

26 J. Li, H. Chen, X. Li, M. Wang, X. Zhang, J. Cao, F. Shen, Y. Wu, S. Xu and H. Fan, Differing toxicity of ambient particulate matter (PM) in global cities, *Atmos. Environ.*, 2019, **212**, 305–315.

27 A. K. Lee, C. K. Chan, M. Fang and A. P. Lau, The 3-hydroxy fatty acids as biomarkers for quantification and characterization of endotoxins and Gram-negative bacteria in atmospheric aerosols in Hong Kong, *Atmos. Environ.*, 2004, **38**, 6307–6317.

28 D. Simazaki, M. Hirose, H. Hashimoto, S. Yamanaka, M. Takamura, J. Watanabe and M. Akiba, Occurrence and fate of endotoxin activity at drinking water purification plants and healthcare facilities in Japan, *Water Res.*, 2018, **145**, 1–11.

29 J. Xue, J. Zhang, B. Xu, J. Xie, W. Wu and Y. Lu, Endotoxins: The Critical Risk Factor in Reclaimed Water *via* Inhalation Exposure, *Environ. Sci. Technol.*, 2016, **50**, 11957–11964.

30 O. Michel, A.-M. Nagy, M. Schroeven, J. Duchateau, J. Neve, P. Fondu and R. Sergysels, Dose-response relationship to inhaled endotoxin in normal subjects, *Am. J. Respir. Crit. Care Med.*, 1997, **156**, 1157–1164.

31 C. Degobbi, P. H. N. Saldiva and C. Rogers, Endotoxin as modifier of particulate matter toxicity: a review of the literature, *Aerobiologia*, 2011, **27**, 97–105.

32 H. Salonen, C. Duchaine, V. Létourneau, M. Mazaheri, S. Laitinen, S. Clifford, R. Mikkola, S. Lappalainen, K. Reijula and L. Morawska, Endotoxin levels and contribution factors of endotoxins in resident, school, and office environments—a review, *Atmos. Environ.*, 2016, **142**, 360–369.

33 H. Salonen, C. Duchaine, V. r. Létourneau, M. Mazaheri, S. Clifford and L. Morawska, Endotoxins in indoor air and settled dust in primary schools in a subtropical climate, *Environ. Sci. Technol.*, 2013, **47**, 9882–9890.

34 T. R. Martin, Recognition of bacterial endotoxin in the lungs, *Am. J. Respir. Cell Mol. Biol.*, 2000, **23**, 128–132.

35 J. Xue, J. Zhang, J. Qiao and Y. Lu, Effects of chlorination and combined UV/Cl2 treatment on endotoxin activity and inhalation toxicity of lipopolysaccharide, gram-negative bacteria and reclaimed water, *Water Res.*, 2019, **155**, 124–130.

36 C. Wang, S. Lu and Z. Zhang, Inactivation of airborne bacteria using different UV sources: Performance modeling, energy utilization, and endotoxin degradation, *Sci. Total Environ.*, 2019, **655**, 787–795.

37 M. Upmann and C. Bonaparte, in *Encyclopedia of Food Microbiology*, ed. R. K. Robinson, Elsevier, Oxford, 1999, pp. 1887–1895, DOI: 10.1006/rwfm.1999.1320.

38 M.-J. Wu, Y.-S. Feng, W.-P. Sung and R. Y. Surampalli, Quantification and Analysis of Airborne Bacterial Characteristics in a Nursing Care Institution, *J. Air Waste Manage. Assoc.*, 2011, **61**, 732–739.

39 I. Rosas, E. Salinas, A. Yela, E. Calva, C. Eslava and A. Cravioto, Escherichia coli in settled-dust and air samples collected in residential environments in Mexico City, *Appl. Environ. Microbiol.*, 1997, **63**, 4093–4095.

40 C. Wang, Z. Zhang and H. Liu, Microwave-induced release and degradation of airborne endotoxins from Escherichia coli bioaerosol, *J. Hazard. Mater.*, 2019, **366**, 27–33.

41 A. P. Castellanos-Arevalo, D. A. Camarena-Pozos, D. C. Castellanos-Arévalo, A. A. Rangel-Córdova, J. J. Peña-Cabriales, B. Arévalo-Rivas, D. G. de Peña and M. Maldonado-Vega, Microbial contamination in the indoor environment of tanneries in Leon, Mexico, *Indoor Built Environ.*, 2016, **25**, 524–540.

42 S. K. Remold, M. E. Purdy-Gibson, M. T. France and T. C. Hundley, Pseudomonas putida and Pseudomonas fluorescens species group recovery from human homes varies seasonally and by environment, *PLoS One*, 2015, **10**, e0127704.

43 Z. Liang, W. L. Chan, X. Tian, A. C. K. Lai, P. K. H. Lee and C. K. Chan, Inactivation of Escherichia coli in droplets at different ambient relative humidities: Effects of phase transition, solute and cell concentrations, *Atmos. Environ.*, 2022, **280**, 119066.

44 Y. Lu, H. Wu, H. Zhang, W. Li and A. Lai, Synergistic disinfection of aerosolized bacteria and bacteriophage by far-UVC (222-nm) and negative air ions, *J. Hazard. Mater.*, 2023, **441**, 129876.

45 H. Zhang, X. Jin, S. S. Nunayon and A. C. K. Lai, Disinfection by in-duct ultraviolet lamps under different environmental conditions in turbulent airflows, *Indoor Air*, 2020, **30**, 500–511.

46 Z. Peng, D. A. Day, G. Symonds, O. Jenks, H. Stark, A. V. Handschy, J. de Gouw and J. L. Jimenez, Significant Production of Ozone from Germicidal UV Lights at 222 nm, *medRxiv*, 2023, preprint, DOI: 10.1101/2023.05.13.23289946.

47 Z. Liang, L. Zhou, R. A. Infante Cuevas, X. Li, C. Cheng, M. Li, R. Tang, R. Zhang, P. K. H. Lee, A. C. K. Lai and C. K. Chan, Sulfate Formation in Incense Burning Particles: A Single-Particle Mass Spectrometric Study, *Environ. Sci. Technol. Lett.*, 2022, **9**, 718–725.

48 J. Degois, M.-E. Dubuis, N. Turgeon, M. Veillette and C. Duchaine, Condensation sampler efficiency for the recovery and infectivity preservation of viral bioaerosols, *Aerosol Sci. Technol.*, 2021, **55**, 653–664.

49 H. Huang, Q.-Y. Wu, Y. Yang and H.-Y. Hu, Effect of chlorination on endotoxin activities in secondary sewage effluent and typical Gram-negative bacteria, *Water Res.*, 2011, **45**, 4751–4757.

50 J. Zhang, J. Xue, B. Xu, J. Xie, J. Qiao and Y. Lu, Inhibition of lipopolysaccharide induced acute inflammation in lung by chlorination, *J. Hazard. Mater.*, 2016, **303**, 131–136.

51 J. Jorgensen, J. Lee, G. Alexander and H. Wolf, Comparison of Limulus assay, standard plate count, and total coliform count for microbiological assessment of renovated wastewater, *Appl. Environ. Microbiol.*, 1979, **37**, 928–931.

52 K. F. Bayston and J. Cohen, Bacterial endotoxin and current concepts in the diagnosis and treatment of endotoxaemia, *J. Med. Microbiol.*, 1990, **31**, 73–83.
53 R. N. Apte, D. H. Pluznik and C. Galanos, Lipid A, the active part of bacterial endotoxins in inducing serum colony stimulating activity and proliferation of splenic granulocyte/macrophage progenitor cells, *J. Cell. Physiol.*, 1976, **87**, 71–78.
54 J. Niemetz and D. Morrison, Lipid A as the biologically active moiety in bacterial endotoxin (LPS)- initiated generation of procoagulant activity by peripheral blood leukocytes, *Blood*, 1977, **49**, 947–956.
55 U. Zähringer, B. Lindner and E. T. Rietschel, Chemical structure of lipid A: recent advances in structural analysis of biologically active molecules, *Endotoxin in Health and Disease*, 2020, pp. 93–114.
56 J.-W. Kang, S.-S. Kim and D.-H. Kang, Inactivation dynamics of 222 nm krypton-chlorine excilamp irradiation on Gram-positive and Gram-negative foodborne pathogenic bacteria, *Food Res. Int.*, 2018, **109**, 325–333.
57 M. Clauß, R. Mannesmann and A. Kolch, Photoreactivation of Escherichia coli and Yersinia enterolytica after irradiation with a 222 nm excimer lamp compared to a 254 nm low-pressure mercury lamp, *Acta Hydrochim. Hydrobiol.*, 2005, **33**, 579–584.
58 J. Sun, S. T. Rutherford, T. J. Silhavy and K. C. Huang, Physical properties of the bacterial outer membrane, *Nat. Rev. Microbiol.*, 2022, **20**, 236–248.
59 J. B. Parsons and C. O. Rock, Bacterial lipids: metabolism and membrane homeostasis, *Prog. Lipid Res.*, 2013, **52**, 249–276.
60 Y.-M. Zhang and C. O. Rock, Membrane lipid homeostasis in bacteria, *Nat. Rev. Microbiol.*, 2008, **6**, 222–233.
61 K. Narita, K. Asano, K. Naito, H. Ohashi, M. Sasaki, Y. Morimoto, T. Igarashi and A. Nakane, Ultraviolet C light with wavelength of 222 nm inactivates a wide spectrum of microbial pathogens, *J. Hosp. Infect.*, 2020, **105**, 459–467.
62 M. Clauß, Higher effectiveness of photoinactivation of bacterial spores, UV resistant vegetative bacteria and mold spores with 222 nm compared to 254 nm wavelength, *Acta Hydrochim. Hydrobiol.*, 2006, **34**, 525–532.
63 J.-W. Ha, J.-I. Lee and D.-H. Kang, Application of a 222-nm krypton-chlorine excilamp to control foodborne pathogens on sliced cheese surfaces and characterization of the bactericidal mechanisms, *Int. J. Food Microbiol.*, 2017, **243**, 96–102.
64 Z. Jing, Z. Lu, D. Santoro, Z. Zhao, Y. Huang, Y. Ke, X. Wang and W. Sun, Which UV wavelength is the most effective for chlorine-resistant bacteria in terms of the impact of activity, cell membrane and DNA?, *Chem. Eng. J.*, 2022, **447**, 137584.
65 A. L. Santos, C. Moreirinha, D. Lopes, A. C. Esteves, I. Henriques, A. Almeida, M. R. M. Domingues, I. Delgadillo, A. Correia and Â. Cunha, Effects of UV Radiation on the Lipids and Proteins of Bacteria Studied by Mid-Infrared Spectroscopy, *Environ. Sci. Technol.*, 2013, **47**, 6306–6315.
66 T. P. Coohill and J. L. Sagripanti, Overview of the inactivation by 254 nm ultraviolet radiation of bacteria with particular relevance to biodefense, *Photochem. Photobiol.*, 2008, **84**, 1084–1090.
67 K. A. Szychowski, K. Rybczyńska-Tkaczyk, M. L. Leja, A. K. Wójtowicz and J. Gmiński, Tetrabromobisphenol A (TBBPA)-stimulated reactive oxygen species (ROS) production in cell-free model using the 2′,7′-dichlorodihydrofluorescein diacetate (H2DCFDA) assay—limitations of method, *Environ. Sci. Pollut. Res.*, 2016, **23**, 12246–12252.
68 D. B. Zorov, M. Juhaszova and S. J. Sollott, Mitochondrial ROS-induced ROS release: an update and review, *Biochim. Biophys. Acta – Bioenerg.*, 2006, **1757**, 509–517.
69 B. D. Needham, S. M. Carroll, D. K. Giles, G. Georgiou, M. Whiteley and M. S. Trent, Modulating the innate immune response by combinatorial engineering of endotoxin, *Proc. Natl. Acad. Sci.*, 2013, **110**, 1464–1469.
70 E. T. Rietschel, T. Kirikae, F. U. Schade, U. Mamat, G. Schmidt, H. Loppnow, A. J. Ulmer, U. Zähringer, U. Seydel, F. Di Padova, M. Schreier and H. Brade, Bacterial endotoxin: molecular relationships of structure to activity and function, *FASEB J.*, 1994, **8**, 217–225.
71 B. Ma, P. M. Gundy, C. P. Gerba, M. D. Sobsey and K. G. Linden, UV Inactivation of SARS-CoV-2 across the UVC Spectrum: KrCl* Excimer, Mercury-Vapor, and Light-Emitting-Diode (LED) Sources, *Appl. Environ. Microbiol.*, 2021, **87**, e01532.
72 R. Xie, G. Y. Tse, L. C. Man, A. L. Cheung, D. T. Wong, E. H. Lam, H. Huang and D. Y. Leung, Systematical Investigations on Disinfection Effectiveness of Far-UVC (222 nm) Irradiation: From Laboratory Study to Field Tests, *J. Appl. Environ. Microbiol.*, 2022, **10**, 17–34.
73 Z. Liang, Y. Chu, M. Gen and C. K. Chan, Single-particle Raman spectroscopy for studying physical and chemical processes of atmospheric particles, *Atmos. Chem. Phys.*, 2022, **22**, 3017–3044.
74 U. K. Krieger, C. Marcolli and J. P. Reid, Exploring the complexity of aerosol particle properties and processes using single particle techniques, *Chem. Soc. Rev.*, 2012, **41**, 6631–6662.
75 A. K. Lee, T. Ling and C. K. Chan, Understanding hygroscopic growth and phase transformation of aerosols using single particle Raman spectroscopy in an electrodynamic balance, *Faraday Discuss.*, 2008, **137**, 245–263.
76 S. N. Ho, Intracellular water homeostasis and the mammalian cellular osmotic stress response, *J. Cell. Physiol.*, 2006, **206**, 9–15.
77 M. Shiraiwa, Y. Li, A. P. Tsimpidi, V. A. Karydis, T. Berkemeier, S. N. Pandis, J. Lelieveld, T. Koop and U. Pöschl, Global distribution of particle phase state in atmospheric secondary organic aerosols, *Nat. Commun.*, 2017, **8**, 1–7.
78 M. Shiraiwa, A. Zuend, A. K. Bertram and J. H. Seinfeld, Gas–particle partitioning of atmospheric aerosols: interplay of

physical state, non-ideal mixing and morphology, *Phys. Chem. Chem. Phys.*, 2013, **15**, 11441–11453.

79 Y. Kaiki, H. Kitagawa, T. Hara, T. Nomura, K. Omori, N. Shigemoto, S. Takahashi and H. Ohge, Methicillin-resistant Staphylococcus aureus contamination of hospital-use-only mobile phones and efficacy of 222-nm ultraviolet disinfection, *Am. J. Infect. Control*, 2021, **49**, 800–803.

80 D. Wang, T. Oppenländer, M. G. El-Din and J. R. Bolton, Comparison of the disinfection effects of vacuum-UV (VUV) and UV light on Bacillus subtilis spores in aqueous suspensions at 172, 222 and 254 nm, *Photochem. Photobiol.*, 2010, **86**, 176–181.

81 D. Welch, M. Buonanno, A. G. Buchan, L. Yang, K. D. Atkinson, I. Shuryak and D. J. Brenner, Inactivation Rates for Airborne Human Coronavirus by Low Doses of 222 nm Far-UVC Radiation, *Viruses*, 2022, **14**, 684.

82 A. Adhikari, E. M. Kettleson, S. Vesper, S. Kumar, D. L. Popham, C. Schaffer, R. Indugula, K. Chatterjee, K. K. Allam, S. A. Grinshpun and T. Reponen, Dustborne and airborne Gram-positive and Gram-negative bacteria in high *versus* low ERMI homes, *Sci. Total Environ.*, 2014, **482–483**, 92–99.

83 R. Balasubramanian, P. Nainar and A. Rajasekar, Airborne bacteria, fungi, and endotoxin levels in residential microenvironments: a case study, *Aerobiologia*, 2012, **28**, 375–390.

84 Z. Fang, C. Gong, Z. Ouyang, P. Liu, L. Sun and X. Wang, Characteristic and Concentration Distribution of Culturable Airborne Bacteria in Residential Environments in Beijing, China, *Aerosol Air Qual. Res.*, 2014, **14**, 943–953.

85 Z. Prazmo, J. Dutkiewicz, C. Skorska, J. Sitkowska and G. Cholewa, Exposure to airborne Gram-negative bacteria, dust and endotoxin in paper factories, *Ann. Agric. Environ. Med.*, 2003, **10**(1), 93–100.

86 D.-U. Park, J.-K. Yeom, W. J. Lee and K.-M. Lee, Assessment of the levels of airborne bacteria, gram-negative bacteria, and fungi in hospital lobbies, *Int. J. Environ. Res. Public Health*, 2013, **10**, 541–555.

87 S. H. Hwang, I. M. Lee and C. S. Yoon, Levels of total airborne bacteria, gram-negative bacteria, and endotoxin according to biosafety levels in Korean biosafety laboratories, *Hum. Ecol. Risk Assess.*, 2013, **19**, 1576–1585.

88 Z. A. Nasir, V. Mula, J. Stokoe, I. Colbeck and M. Loeffler, Evaluation of total concentration and size distribution of bacterial and fungal aerosol in healthcare built environments, *Indoor Built Environ.*, 2015, **24**, 269–279.

89 S. H. Mirhoseini, M. Didehdar, M. Akbari, R. Moradzadeh, R. Jamshidi and S. Torabi, Indoor exposure to airborne bacteria and fungi in sensitive wards of an academic pediatric hospital, *Aerobiologia*, 2020, **36**, 225–232.

90 B. A. Zucker, S. Trojan and W. Müller, Airborne Gram-negative bacterial flora in animal houses, *J. Vet. Med., Ser. B*, 2000, **47**, 37–46.

91 C. Chang, H. Chung, C.-F. Huang and H.-J. J. Su, Exposure of workers to airborne microorganisms in open-air swine houses, *Appl. Environ. Microbiol.*, 2001, **67**, 155–161.

92 J. Dutkiewicz, Z. J. Pomorski, J. Sitkowska, E. Krysińska-Traczyk, C. Skórska, Z. Prażmo, G. Cholewa and H. Wójtowicz, Airborne microorganisms and endotoxin in animal houses, *Grana*, 1994, **33**, 85–90.

93 H. Aydogdu, A. Asan and M. Tatman Otkun, Indoor and outdoor airborne bacteria in child day-care centers in Edirne City (Turkey), seasonal distribution and influence of meteorological factors, *Environ. Monit. Assess.*, 2010, **164**, 53–66.

94 F. Tsai, J. Macher and Y. Hung, Concentrations of airborne bacteria in 100 US office buildings, *Indoor Air*, 2002, **4**, 353–358.

95 F. Tsai and J. Macher, Concentrations of airborne culturable bacteria in 100 large US office buildings from the BASE study, *Indoor air*, 2005, **15**, 71–81.

96 P. Reanprayoon and W. Yoonaiwong, Airborne concentrations of bacteria and fungi in Thailand border market, *Aerobiologia*, 2012, **28**, 49–60.

97 Z. Peng, S. L. Miller and J. L. Jimenez, Model Evaluation of Secondary Chemistry due to Disinfection of Indoor Air with Germicidal Ultraviolet Lamps, *Environ. Sci. Technol. Lett.*, 2022, **10**(1), 6–13.

98 J. P. Abbatt and C. Wang, The atmospheric chemistry of indoor environments, *Environ. Sci.: Processes Impacts*, 2020, **22**, 25–48.

99 C. Wang, D. B. Collins and J. P. D. Abbatt, Indoor Illumination of Terpenes and Bleach Emissions Leads to Particle Formation and Growth, *Environ. Sci. Technol.*, 2019, **53**, 11792–11800.